受入
78-9-85
高工研図書室

DESY 78/36
July 1978
Erratum

QCD Predictions for Jets in e^+e^- Annihilation: Angular Correlations and Asymmetries

by

G. Kramer
II. Institut für Theoretische Physik der Universität Hamburg

G. Schierholz and J. Willrodt
Deutsches Elektronen-Synchrotron DESY, Hamburg

Equations (2) - (4) have been incorrectly transformed into $d\sigma_u/dT$, $d\sigma_L/dT$ and $d\sigma_I/dT$ (case B). Equation (6) should read

$$\frac{d\sigma_u}{dT} = \sigma^{(1)} \left[\frac{2(3T^2-3T+2)}{T(1-T)} \ln \frac{2T-1}{1-T} - \frac{3(3T-2)(2-T)}{1-T} - \frac{2(8T-3T^2-4)}{T^2} \right]$$

$$\frac{d\sigma_L}{dT} = \sigma^{(1)} \frac{2(8T-3T^2-4)}{T^2}$$

$$\frac{d\sigma_T}{dT} = \frac{1}{2} \frac{d\sigma_L}{dT}$$

Case A:

$$\frac{d\sigma_I}{dT} = \sigma^{(1)} \frac{1}{2\sqrt{2}} \left[\frac{2(2-T)(3T-2)\sqrt{2T-1}}{T^2} - \frac{2+T}{\sqrt{1-T}} \arcsin\left(\frac{3T-2}{T}\right) \right]$$

Case B:

$$\frac{d\sigma_I}{dT} = \sigma^{(1)} \sqrt{2} (2-2T+T^2) \left[\frac{2}{T^2} \sqrt{2T-1} - \frac{1}{T\sqrt{1-T}} \right] \quad (6)$$

This invalidates Fig. 4 and Equations (8) and (9). Figure 4 is corrected here. Equations (8) and (9) should read

T = 0.8:

$$\sim 1 + 0.60 \cos^2\theta + 0.10 \sin^2\theta \cos 2\chi \quad (8)$$

$$+ \left\{ \begin{matrix} 0.14 \\ 0.10 \end{matrix} \right\} \sin 2\theta \cos\chi$$

T = 0.75:

$$\sim 1 + 0.44 \cos^2\theta + 0.14 \sin^2\theta \cos 2\chi$$

$$+ \left\{ \begin{matrix} 0.13 \\ 0.08 \end{matrix} \right\} \sin 2\theta \cos\chi \qquad (9)$$

It is no longer true that the asymmetry is largest for case B.

In Eq. (11) it should read

Case B:

$$\sigma_I = \sigma_0 \frac{\alpha_s(q^2)}{\pi} \frac{2\sqrt{2}}{3} \left(-\frac{34}{3} + \frac{16}{\sqrt{3}} + \frac{4}{3}\pi + 2 \ln \frac{\sqrt{3}-1}{\sqrt{3}+1} \right)$$

We like to thank J. Cleymans, M. Kuroda and D. Schiller for drawing our attention to this.

Figure Caption

Fig. 4 Corrected partial cross sections.

$U: d\sigma_U/dT$, $L: d\sigma_L/dT$ and $I: -d\sigma_I/dT$.

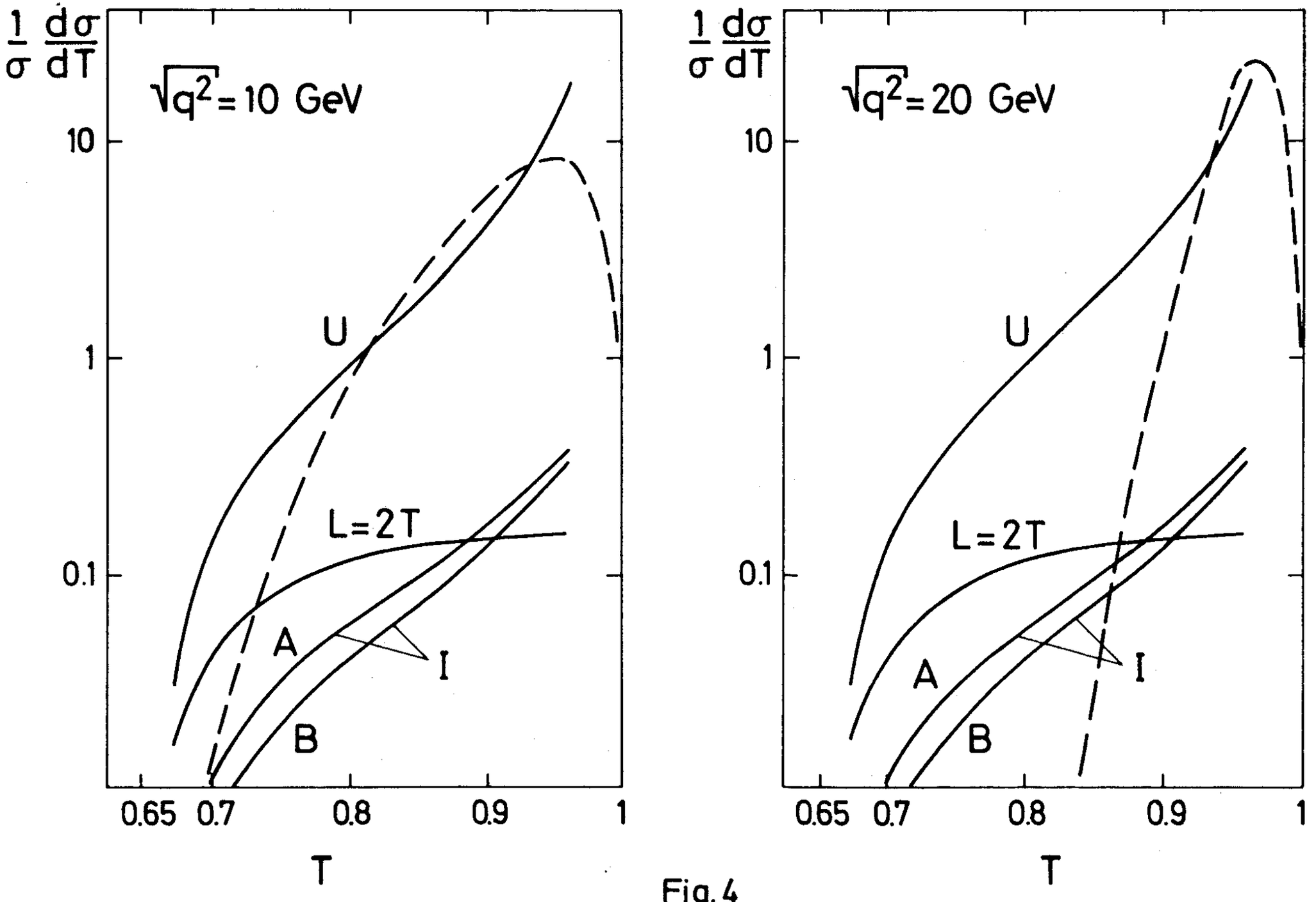
1/σ dσ/dT
√q² = 10 GeV
10
1
0.1
U
L=2T
A
I
B
0.65
0.7
0.8
0.9
1
T
1/σ dσ/dT
√q² = 20 GeV
10
1
0.1
U
L=2T
A
I
B
0.65
0.7
0.8
0.9
1
T

Fig. 4

DEUTSCHES ELEKTRONEN-SYNCHROTRON **DESY**

DESY 78/36
July 1978

受入
78-9-85
高工研図書室

QCD PREDICTIONS FOR JETS IN e^+e^- ANNIHILATION: ANGULAR CORRELATIONS AND ASYMMETRIES

by

G. Kramer
II. Institut für Theoretische Physik der Universität Hamburg

G. Schierholz and J. Willrodt
Deutsches Elektronen-Synchrotron DESY, Hamburg

NOTKESTRASSE 85 · 2 HAMBURG 52

To be sure that your preprints are promptly included in the
HIGH ENERGY PHYSICS INDEX ,
send them to the following address (if possible by air mail) :

DESY
Bibliothek
Notkestrasse 85
2 Hamburg 52
Germany

QCD PREDICTIONS FOR JETS IN e^+e^- ANNIHILATION: ANGULAR CORRELATIONS AND ASYMMETRIES

by

G. Kramer
II. Institut für Theoretische Physik der Universität Hamburg

G. Schierholz and J. Willrodt
Deutsches Elektronen-Synchrotron DESY, Hamburg

Abstract:

The topological features of hadron jets in e^+e^- annihilation may reliably be calculated in QCD perturbation theory. To second order the final state hadrons fall into quark-antiquark and quark-antiquark-gluon initiated jets. The latter induce angular asymmetries which are extensively studied.

Quantum chromodynamics (QCD) stands a good chance to be the underlying theory of the strong interactions. Qualitatively, it receives strong support from recent years' experiments. But this cannot hide the fact that quantitative evidence is still scarce.

It is impressive how well QCD accounts for the scaling violations seen in deep inelastic lepton hadron scattering.[1] But, as has been pointed out elsewhere,[2] most of the scaling violations also allow a conventional explanation in terms of new thresholds (e.g., charm) opening up in going to higher energies[2] and certain (dynamical) scale breaking effects showing up in the twist- 6 (and higher) operators in the operator product expansion.[3] This indicates that a quantitative test of QCD at present energies and for space-like photons is very much aggravated by nonperturbative binding corrections which can at best be estimated.

This situation is likely to change for high energy electron-positron annihilation into hadrons at PETRA and PEP. Firstly, it is conceivable that for a wide range of q^2 (say for q^2 between $\sim$ 100 GeV^2 and $\sim$1000 GeV^2) no new flavour degree of freedom will be excited which eliminates this source of ambiguity. Secondly, there is a wide range of partial cross sections which can be calculated perturbatively in QCD and hence do not suffer from intractable details of hadronic bound states. This makes PETRA and PEP an ideal place to search for unmistakable QCD signals.

Sterman and Weinberg[4] have argued that the absence of mass singularities be taken as a criterion for the validity of perturbation theory. This criterion is satisfied if we limit our considerations to final state measurements which do not entail the properties of specific hadrons. Such quantities are, e.g., the (various) total cross sections[+] and distinctive features of hadronic jets.

In this letter we shall give full account of the topology of hadron jets in e^+e^- annihilation in lowest nontrivial order of perturbation theory. In

[+] I.e., σ_U, σ_L, σ_T and σ_I.

particular, we predict a sizable angular correlation between the plane of the jets, originating from the hard gluon bremsstrahlung correction, and the beam axis, being a direct test of QCD.

To order $g^2/4\pi$, g being the quark-gluon coupling constant, hard gluon bremsstrahlung (Fig.1b and 1c) gives rise to three jet events while the rest of the cross section corresponds to two jets. The average transverse momentum of the $q\bar{q}g$ final state grows like $(q^2/\ln(q^2/\Lambda^2))^{1/2}$. While it is usually assumed, with reference to the parton model, that the (non-perturbative) quark and gluon fragmentation into hadron is characterized by a limited $\langle p_\perp \rangle \simeq 400$ MeV , this becomes negligible with respect to the transverse momentum of each jet at high energies so that a distinct signal of primary $q\bar{q}g$ production should emerge.

Following Sterman and Weinberg,[4] various authors[5)6)] have proposed variables for measuring the jet topology which are infrared insensitive and, hence, can be reliably calculated in QCD perturbation theory. Among those are thrust T, spherocity S and acoplanarity A.

For algebraic convenience we shall put the quark mass equal to zero[+]. For unpolarized electrons and positrons the functional form of the basic partial cross section for $e^+e^- \to \gamma^* \to q(p_1)\bar{q}(p_2)g(p_3)$ is given by[8]

$$2\pi \frac{d^4\sigma}{d\cos\theta\, d\chi\, dx_1 dx_2} = \frac{3}{8}(1+\cos^2\theta)\frac{d^2\sigma_U}{dx_1 dx_2} + \frac{3}{4}\sin^2\theta \frac{d^2\sigma_L}{dx_1 dx_2} + \frac{3}{4}\sin^2\theta\cos 2\chi \frac{d^2\sigma_T}{dx_1 dx_2} - \frac{3}{2\sqrt{2}}\sin 2\theta\cos\chi \frac{d^2\sigma_I}{dx_1 dx_2} \quad (1)$$

[+] Our results for massive quarks will be published elsewhere.[7]

where $x_i = 2\,p_i/\sqrt{q^2}$ $(x_1 + x_2 + x_3 = 2)$. Θ is the angle between the incoming electron beam and the thrust axis while χ is the azimuthal angle between the $q\bar{q}g$ -production plane and the beam axis (Fig.2). The thrust axis coincides with the direction of the maximum momentum which can be carried by either quark, antiquark or gluon.

The cross sections σ_U, σ_L, σ_T and σ_I have the following interpretation. $\sigma_U(\sigma_L)$ is the cross section for unpolarized transverse (longitudinally polarized) photons with helicity axis $\vec{Oz}$, i.e., the thrust axis (Fig.2). σ_T (σ_I) corresponds to the interference of helicity + 1 and - 1 amplitudes (the real part of helicity + 1 and 0 interference).

In calculating the various partial cross sections we have to distinguish between three kinematical regions (Fig.3):

I: $x_1 > x_2, x_3$

II: $x_2 > x_1, x_3$

III: $x_3 > x_1, x_2$

In region I(II) the thrust axis coincides with the direction of the outgoing quark (antiquark) while in region III the thrust axis corresponds to the gluon momentum.

In the various regions we find

I:

$$\frac{d^2\sigma_U}{dx_1\,dx_2} = \sigma^{(1)}\,\frac{1}{(1-x_1)(1-x_2)}\left[x_1^2 + x_2^2\left(1-\tfrac{1}{2}\sin^2\theta_{12}\right)\right]$$

$$\frac{d^2\sigma_L}{dx_1\,dx_2} = \sigma^{(1)}\,\frac{1}{(1-x_1)(1-x_2)}\,\tfrac{1}{2}x_2^2\sin^2\theta_{12} \qquad (2)$$

$$\frac{d^2\sigma_T}{dx_1\,dx_2} = \tfrac{1}{2}\,\frac{d^2\sigma_L}{dx_1\,dx_2}$$

$$\frac{d^2\sigma_I}{dx_1\,dx_2} = \sigma^{(1)}\,\frac{1}{(1-x_1)(1-x_2)}\,\frac{1}{4\sqrt{2}}\,x_2^2\sin 2\theta_{12}$$

II:

$$\frac{d^2\sigma_U}{dx_1\,dx_2} = \sigma^{(1)}\frac{1}{(1-x_1)(1-x_2)}\left[x_2^2 + x_1^2\left(1-\tfrac{1}{2}\sin^2\theta_{12}\right)\right]$$

$$\frac{d^2\sigma_L}{dx_1\,dx_2} = \sigma^{(1)}\frac{1}{(1-x_1)(1-x_2)}\,\tfrac{1}{2}\,x_1^2\sin^2\theta_{12} \qquad (3)$$

$$\frac{d^2\sigma_T}{dx_1\,dx_2} = \frac{1}{2}\,\frac{d^2\sigma_L}{dx_1\,dx_2}$$

$$\frac{d^2\sigma_I}{dx_1\,dx_2} = \sigma^{(1)}\frac{1}{(1-x_1)(1-x_2)}\,\frac{1}{4\sqrt{2}}\,x_1^2\sin 2\theta_{12}$$

III:

$$\frac{d^2\sigma_U}{dx_1\,dx_2} = \sigma^{(1)}\frac{1}{(1-x_1)(1-x_2)}\left[x_1^2\left(1-\tfrac{1}{2}\sin^2\theta_{13}\right) + x_2^2\left(1-\tfrac{1}{2}\sin^2\theta_{23}\right)\right]$$

$$\frac{d^2\sigma_L}{dx_1\,dx_2} = \sigma^{(1)}\frac{1}{(1-x_1)(1-x_2)}\left[x_1^2\sin^2\theta_{13} + x_2^2\sin^2\theta_{23}\right]$$

$$\frac{d^2\sigma_T}{dx_1\,dx_2} = \frac{1}{2}\,\frac{d^2\sigma_L}{dx_1\,dx_2} \qquad (4)$$

$$\frac{d^2\sigma_I}{dx_1\,dx_2} = \sigma^{(1)}\frac{1}{(1-x_1)(1-x_2)}\,\frac{1}{4\sqrt{2}}\left[x_1^2\sin 2\theta_{13} + x_2^2\sin 2\theta_{23}\right]$$

where $\sigma^{(1)} = \frac{2}{3} \frac{g^2}{4\pi^2} \sigma_0$, σ_0 being the cross section for $e^+e^- \to q\bar{q}$ in Born approximation, and

$$\begin{aligned} \cos\theta_{12} &= 1 + \frac{2}{x_1 x_2}(1-x_1-x_2) \\ \cos\theta_{13} &= 1 + \frac{2}{x_1 x_3}(1-x_1-x_3) \\ \cos\theta_{23} &= 1 + \frac{2}{x_2 x_3}(1-x_2-x_3) \end{aligned} \tag{5}$$

Along with the definition of angles (Fig.2) θ_{12}, θ_{13} and θ_{23} will range between $0 \leq \theta_{12} \leq \pi$, $0 \leq \theta_{13} \leq \pi$ and $\pi \leq \theta_{23} \leq 2\pi$.

It is easy to see that σ_L, σ_T and σ_I are infrared finite ($\sin^2\theta_{ij} \sim (1-x_1)(1-x_2)$). The infrared divergence inherent in σ_U cancels with the infrared singularity arising from the interference between diagram 1a and the Born term.

We are now ready to give the results for the differential cross sections in, e.g., thrust and spherocity.[+)] Here we shall mainly be interested in the thrust distribution which means to integrate (2), (3) and (4) over their appropriate regions keeping x_1, x_2 and $x_3 = 2 - x_1 - x_2$, respectively, fixed. Since one measures hadrons and not quarks and gluons we also need to specify the azimuthal angle χ (Fig.2) in terms of observable quantities. Note that it is the term proportional to $\cos\chi$ in the angular distribution (1) which, being asymmetric in $\chi \to \chi + \pi$ (i.e., $\vec{Ox} \to -\vec{Ox}$), makes a proper definition of χ necessary.

Two choices come to our mind:

A. We distinguish gluon jets from quark and antiquark jets, the latter not

---

[+)] Note that $A = 0$ for $e^+e^- \to q\bar{q}g$. Spherocity will not be a useful quantity for analyzing three-jet events as we shall see later on.

being differentiated.[+)] This should be feasible since we expect the gluon jet to have, e.g., a much higher multiplicity.[++)] We then choose $-\vec{Ox}$ to point into the direction of the gluon jet. In other words, $\vec{Ox}$ defines the hemisphere in which to find the quark (region I) and antiquark jet (region II), respectively. In this case σ_I does not receive any contribution from region III, i.e., where the gluon is most energetic.

B. We choose $\vec{Ox}$ to point into the hemisphere in which to find the second most energetic jet originating either from a quark, antiquark or gluon.

Clearly, A and B will only affect σ_I. For the various partial cross sections we find

$$\frac{d\sigma_U}{dT} = \sigma^{(1)} \left[\frac{2(3T^2-3T+2)}{T(1-T)} \ln\frac{2T-1}{1-T} - 4\ln\frac{T}{2(1-T)} - \frac{3(3T-2)(2-T)}{1-T} + \frac{(3T-2)^2}{T^2} \right]$$

$$\frac{d\sigma_L}{dT} = \sigma^{(1)} \left[4\ln\frac{T}{2(1-T)} - \frac{(3T-2)^2}{T^2} \right]$$

$$\frac{d\sigma_T}{dT} = \frac{1}{2}\frac{d\sigma_L}{dT} \qquad (6)$$

Case A:

$$\frac{d\sigma_I}{dT} = \sigma^{(1)} \frac{1}{2\sqrt{2}} \left[\frac{2(2-T)(3T-2)\sqrt{2T-1}}{T^2} - \frac{2+T}{\sqrt{1-T}} \arcsin\left(\frac{3T-2}{T}\right) \right]$$

Case B:

$$\frac{d\sigma_I}{dT} = \sigma^{(1)} \sqrt{2} \left[\frac{4(1-T)^2\sqrt{2T-1}}{T^2} - \frac{2T-1}{T\sqrt{1-T}} \right]$$

[+)] Topologically, quark and antiquark jets look the same.

[++)] Following simply from the fact that the gluon fragmentation function has a stronger threshold factor than the quark fragmentation function. See also Ref.9.

Again, the infrared singularity ($T \to 1$) of σ_U cancels against the infrared singularity in $e^+e^- \to q\bar{q}$ to order g^2. In comparing (6) with results stated elsewhere it should be noted that $\sigma(e^+e^- \to q\bar{q}g) = \sigma_U + \sigma_L$.

For the $q\bar{q}g$ final state T varies between $\frac{2}{3} \leq T \leq 1$. The cross section for $e^+e^- \to q\bar{q}$, on the other hand, is $d\sigma/dT \sim \delta(1 - t)$ so that for smaller T the three-jet configuration should stick out. For finite energies the T distribution will, however, be smeared out by the quark and gluon fragmentation which takes place at non-zero, though limited $p_\perp$.

We identify $g^2/4\pi$ with the renormalization group running coupling constant. For five quark flavours this yields

$$\frac{g^2}{4\pi} \equiv \alpha_s(q^2) = \frac{1.64}{\ln(q^2/\Lambda^2)} \qquad (7)$$

where Λ is determined to be [+)] $\Lambda \simeq$ 700 MeV. In Fig.4 we have plotted the various partial cross sections (6) divided by the total cross section (to order α_s). Also shown is the cross section $d\sigma(e^+e^- \to q\bar{q})/dT$ folded with the experimental quark fragmentation function[6)] for 10 and 20 GeV.

If QCD is the correct underlying theory, we predict that all events with not too large T (e.g., $T \lesssim 0.85$ for 20 GeV) will be oblate and vary in shape between a pan with the panhandle being the thrust axis and a three-toothed star with less distinct thrust axis. The thrust axis and the production plane with either of the two definitions, A and B, of $\vec{Ox}$ (Fig.2) will be distributed according to (1) with $d^2\sigma_\lambda/dx_1\,dx_2$ (λ = U, L, T, I) replaced by[++)] $d\sigma_\lambda/dT$.

[+)] E.g., Ref.10. This value agrees with the most recent analysis of the CERN neutrino cross section.[11)] Moorehouse et al.[12)] obtain a somewhat smaller value.

[++)] The coefficients of the various angular parts can be directly read off from Fig.4 multiplying $d\sigma_L/dT$ ($d\sigma_T/dT$) by $2(2\sqrt{2})$.

Explicitly, we find for moderate T

T = 0.8:

$$\sim 1 + 0.38 \cos^2\Theta + 0.16 \sin^2\Theta \cos 2\chi + \left\{\begin{matrix}0.08\\0.37\end{matrix}\right\} \sin 2\Theta \cos\chi \qquad (8)$$

T = 0.75:

$$\sim 1 + 0.28 \cos^2\Theta + 0.18 \sin^2\Theta \cos 2\chi + \left\{\begin{matrix}0.13\\0.48\end{matrix}\right\} \sin 2\Theta \cos\chi \qquad (9)$$

where the upper (lower) value corresponds to the definition A (B).

Equations (8) and (9) indicate a substantial deviation from the $1 + \cos^2\Theta$ distribution of the thrust axis as predicted by the parton model. The term proportional to $\cos 2\chi$, describing the azimuthal correlation of the jet plane with respect to the beam axis, predicts the jet plane to preferentially form a small angle with the beam axis, i.e., $-\frac{\pi}{4} < \chi < \frac{\pi}{4}$ or $\frac{3}{4}\pi < \chi < \frac{5}{4}\pi$. As can be deduced from Fig. 4, this effect is most prominant for T near its lower boundary [+)] where $d\sigma_T/dT$ and $d\sigma_U/dT$ become close. The best choice for the polar angle Θ is $\Theta = \frac{\pi}{2}$ where for moderate T we expect a 30 % signal. The last term in the angular distribution formula ($\sim \cos\chi$) provides the most distinctive test of QCD. Measuring this term requires to locate the gluon jet (A) or the jet of second maximal directed momentum (B) within the jet plane. The effect is largest for case B. This suggests to analyze the data in terms of thrust and a suitably defined quantity which determines the axis of the second most energetic jet. We propose to use [++)]

[+)] For the azimuthal correlation $\cos 2\chi$ it does not matter if, experimentally, the thrust axis can be uniquely determined.

[++)] For a more sophisticated discussion see Ref. 13.

$$T_2(\vec{n}_2) = 2 \max_{\vec{n}_2} \frac{\sum_i \vec{p}_i \vec{n}_2 \, \theta(-\vec{p}_i \vec{n}_1)\, \theta(\vec{p}_i [\vec{n}_2 - (\vec{n}_1 \vec{n}_2)\vec{n}_1])}{\sum_i |\vec{p}_i|} \qquad (10)$$

where $\vec{n}_{1,2}$ are unit vectors with $\vec{n}_1$ along the thrust axis. The summation is over the intersection of the hemisphere opposite to the thrust axis ($\vec{p}_i \vec{n}_1 < 0$) and the hemisphere $p_{ix} > 0$, i.e., over those particles which originate in the second most energetic jet (axis $\vec{n}_2$). Evidently, spherocity is not a useful quantity for testing QCD.

Finally we shall be interested in the averaged cross section (over T) $2\pi \, d^2\sigma/d\cos\Theta \, d\alpha$. This has the form (1) with coefficients σ_U , σ_L , σ_T and σ_I . To order α_s we find

$$\sigma_U = \sigma_0 \left[1 + \frac{\alpha_s(q^2)}{\pi} \left(5 - \frac{32}{3} \ln \frac{3}{2} \right) \right]$$

$$\sigma_L = \sigma_0 \frac{\alpha_s(q^2)}{\pi} \left(\frac{32}{3} \ln \frac{3}{2} - 4 \right)$$

$$\sigma_T = \frac{1}{2} \sigma_L \qquad (11)$$

Case A:

$$\sigma_I = \sigma_0 \frac{\alpha_s(q^2)}{\pi} \frac{2\sqrt{2}}{3} \left(\frac{28}{3} - \frac{32}{3\sqrt{3}} - \frac{11}{9}\pi \right)$$

Case B:

$$\sigma_I = \sigma_0 \frac{\alpha_s(q^2)}{\pi} \frac{2\sqrt{2}}{3} \left(\frac{58}{3} - \frac{28}{\sqrt{3}} - 2\pi - 2 \ln \frac{\sqrt{3}-1}{\sqrt{3}+1} \right)$$

where σ_U now also includes the Born term (of $e^+e^- \to \delta^* \to q\bar{q}$) and the second order diagram interfering with the Born term. For $\sqrt{q^2}$ = 20 GeV this gives

$$2\pi \frac{d^2\sigma}{d\cos\theta\, d\chi} = 0.41\,\sigma_0 \left[1 + 0.92\cos^2\theta \right.$$

$$\left. + 0.02\sin^2\theta\cos 2\chi + \begin{Bmatrix} 0.12 \\ 0.09 \end{Bmatrix} \sin 2\theta\cos\chi \right] \qquad (12)$$

where the upper (lower) number corresponds to A (B). The term proportional to cos 2χ will be hard to recognize in the total data sample [+)] while the last term ($\sim \cos\chi$) and the deviation from the $1 + \cos^2\theta$ distribution of the thrust axis should be measurable.

For transversely polarized electrons and positrons the angular distribution is of the form (e.g., Fig. 2)

$$\begin{aligned} 2\pi \frac{d^2\sigma}{d\cos\theta\, d\chi} &= \frac{3}{8}(1+\cos^2\theta + P^2\sin^2\theta\cos 2\phi)\,\sigma_U \\ &+ \frac{3}{4}(1 - P^2\cos 2\phi)\sin^2\theta\,\sigma_L \\ &+ \frac{3}{4}\left[(\sin^2\theta + P^2\cos 2\phi(1+\cos^2\theta))\cos 2\chi \right. \\ &\qquad \left. - 2P^2\sin 2\phi\cos\theta\sin 2\chi \right]\sigma_T \\ &- \frac{3}{\sqrt{2}}\left[(1 - P^2\cos 2\phi)\cos\theta\cos\chi \right. \\ &\qquad \left. + P^2\sin 2\phi\sin\chi \right]\sin\theta\,\sigma_I \end{aligned} \qquad (13)$$

where P is the transverse polarization of each beam. The same formula holds for the partial cross sections. Eventually this will allow to measure σ_U, σ_L, σ_T and σ_I more accurately given the limited acceptance of the detectors.

In our view e^+e^- annihilation into hadrons offers a decisive test of the underlying theory of hadronic physics. Experimentalists should, however, be aware that weak decays of charmed and bottom quarks give rise to a similar asymmetry which is not to be confused.

[+)] After having finished our calculations we became aware of a preprint by Pi, Jaffe and Low [14)] who have also given this number.

References

1) E.g., I. Hinchliffe and C.H. Llewellyn-Smith, Nucl. Phys. B128, 93 (1977); A. De Rujula, H. Georgi and H.D. Politzer, Ann. Phys. 103, 315 (1977); A.J. Buras and K. Gaemers, Nucl. Phys. B132, 249 (1978); see also O. Nachtmann, in Proceedings of the 1977 International Symposium on Lepton and Photon Interactions at High Energies, Hamburg (ed. F. Gutbrod), p. 811.

2) M. Kuroda and G. Schierholz, DESY preprint DESY 78/8 (1978), to be published in Nucl. Phys. B.

3) I.A. Schmidt and R. Blankenbecler, Phys. Rev. D16, 1318 (1977).

4) G. Sterman and S. Weinberg, Phys. Rev. Letters 39, 1436 (1977).

5) H. Georgi and M. Machacek, Phys. Rev. Letters 39, 1237 (1977); E. Farhi, Phys. Rev. Letters 39, 1587.

6) A. De Rujula, J. Ellis, E.G. Floratos and M.K. Gaillard, Nucl. Phys. B138, 387 (1978).

7) G. Kramer, G. Schierholz and J. Willrodt , in preparation.

8) N.M. Avram and D.H. Schiller, Nucl. Phys. B70, 272 (1974); A.C. Hirshfeld and G. Kramer, Nucl. Phys. B74, 211 (1974).

9) K. Koller and T.F. Walsh, Phys. Letters 72B, 227 (1977); Erratum 73B, 504 (1978).

10) R. Shankar, Phys. Rev. D15, 755 (1977).

11) W. Scott, talk presented at the Topical Conference on Neutrino Physics at Accelerators, Oxford, July 1978, to appear in the proceedings.

12) R.G. Moorehouse, M.R. Pennington and G.G. Ross, Nucl. Phys. B124, 285 (1977).

13) S. Brandt and H.D. Dahmen, Siegen preprint SI 78-8 (1978).

14) S.-Y. Pi, R.L. Jaffe and F.E. Low, MIT preprint CTP-715 (1978).

Figure Captions

Fig. 1 Second order QCD diagrams for $e^+e^- \to \gamma^* \to$ hadrons: (a) diagram interfering with the Born graph, (b) and (c) diagrams for gluon production.

Fig. 2 Definition of angles Θ, χ and ϕ. The thrust axis is along $\vec{Oz}$ while the q, $\bar{q}$ and g momenta lie in the plane (x, z). The (y, z) plane divides the final state into two hemispheres. $\vec{Ox}$ defines the hemisphere in which to find the antiquark (quark) in case of the thrust axis being given by the quark (antiquark) momentum. If the gluon is most energetic $\vec{Ox}$ defines the hemisphere in which to find the quark. The angles Θ, χ and ϕ vary between $0 \leq \Theta \leq \pi$, $0 \leq \chi \leq 2\pi$ and $0 \leq \phi \leq 2\pi$. When talking about the thrust distribution $\vec{Ox}$ will be defined according to A and B.

Fig. 3 Regions of integration. For their proper definition see text.

Fig. 4 Partial cross sections. U: $d\sigma_U/dT$, L: $d\sigma_L/dT$ and I: $-d\sigma_I/dT$; $d\sigma_T/dT = 1/2\, d\sigma_L/dT$. The dashed curve shows $d\sigma(e^+e^- \to q\bar{q})/dT$ smeared out by the quark fragmentation functions. This is taken from Ref. 6.

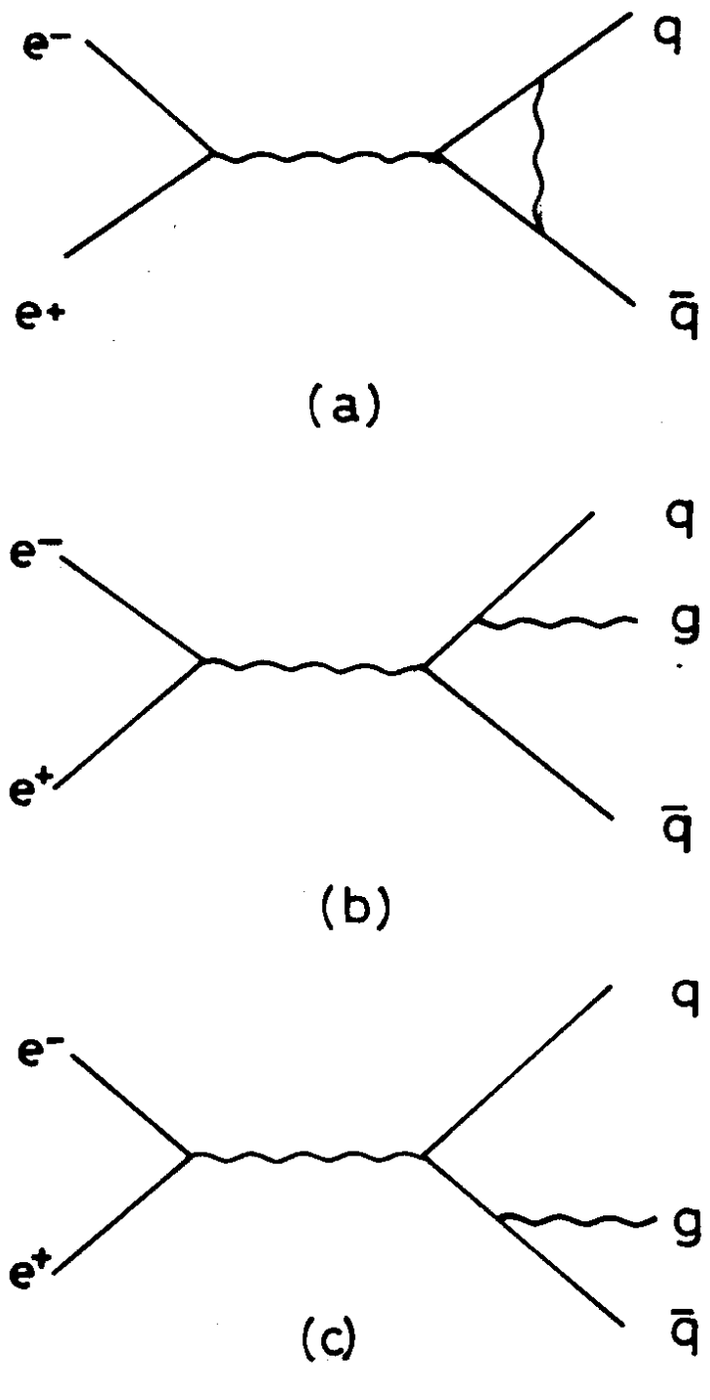

FIG. 1

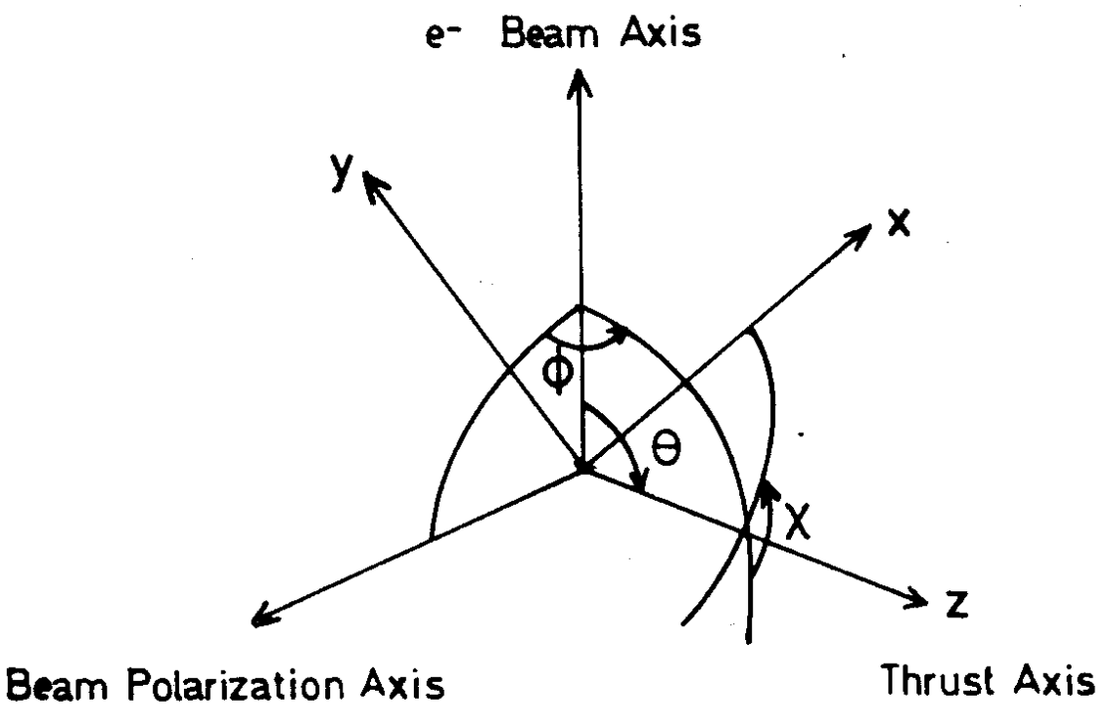

FIG. 2

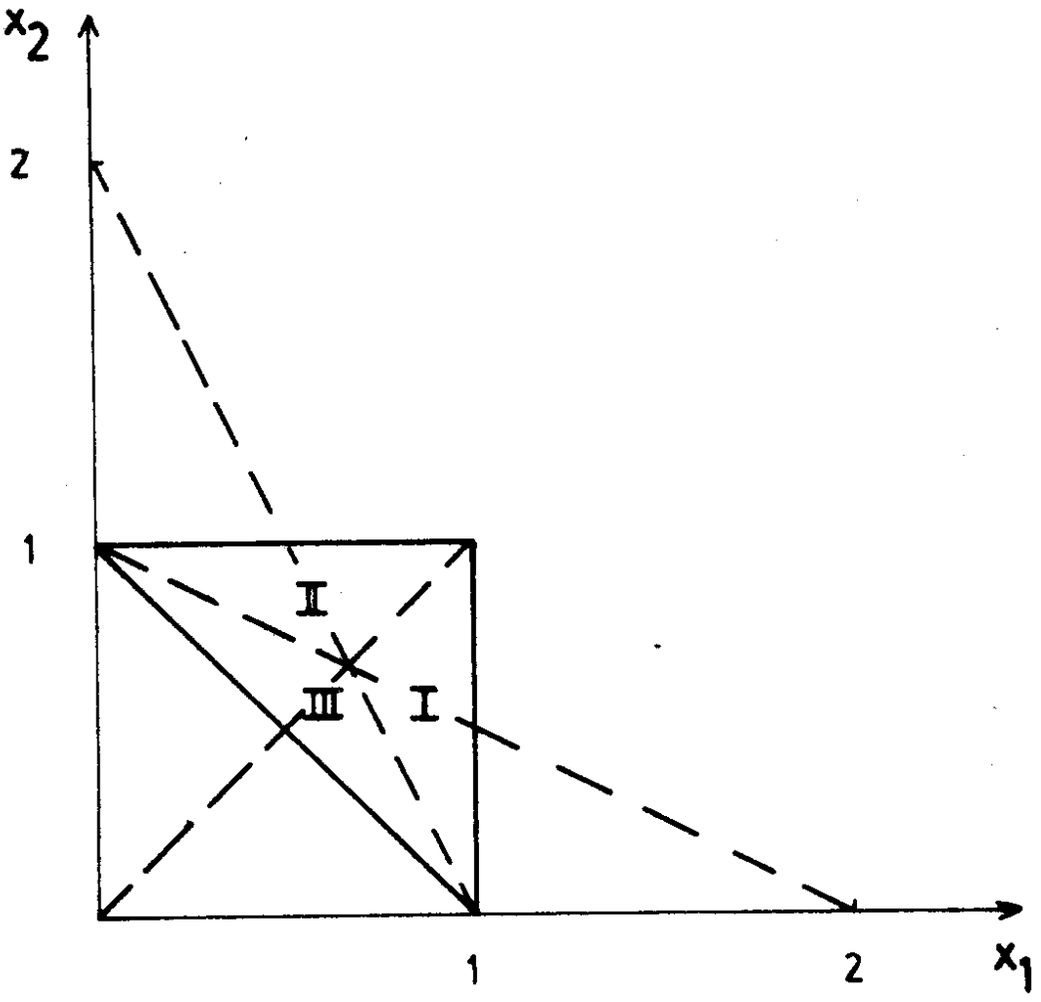

FIG. 3

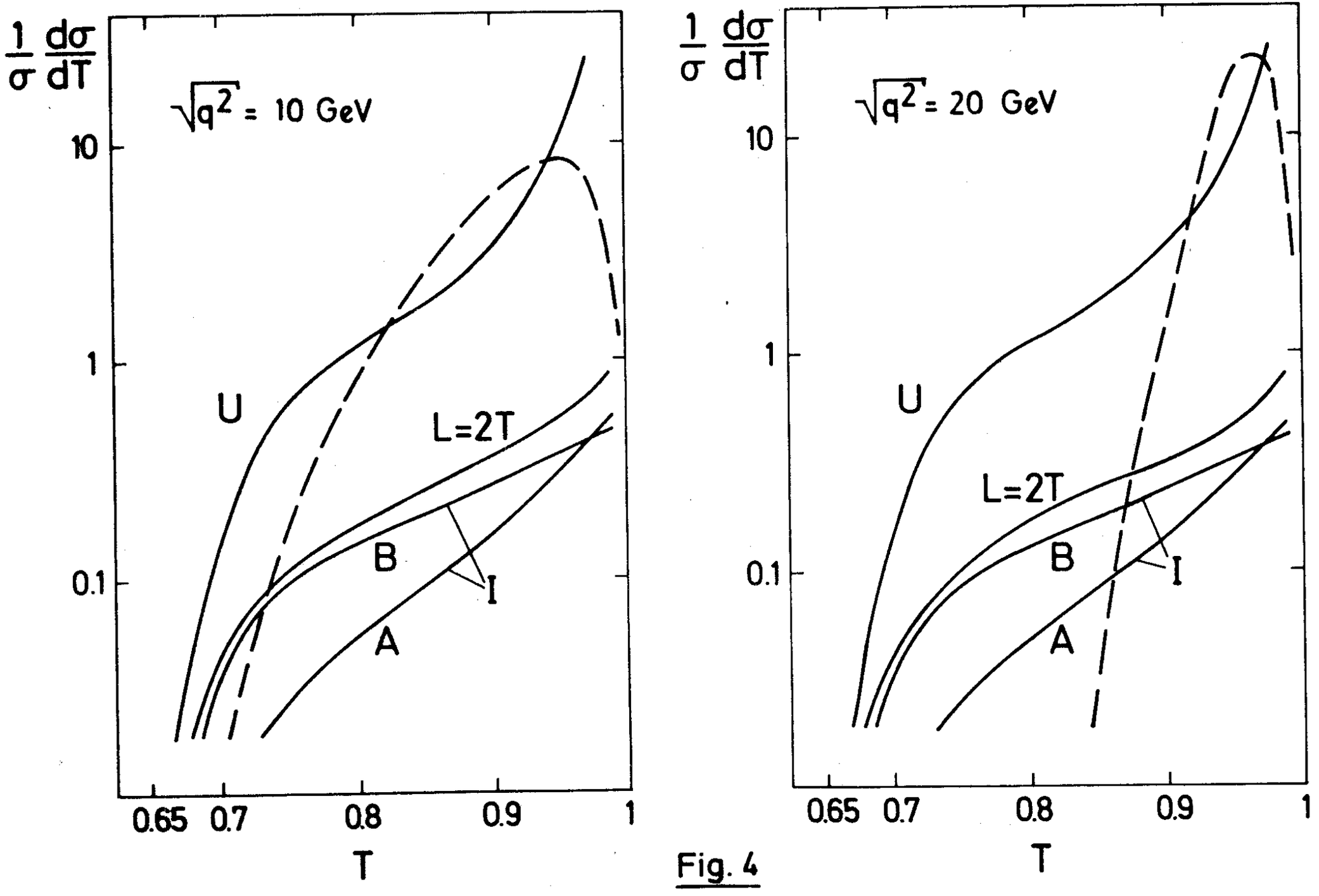
$\frac{1}{\sigma}\frac{d\sigma}{dT}$
$\sqrt{q^2}$ = 10 GeV
10
1
0.1
U
L=2T
B
I
A
0.65
0.7
0.8
0.9
1
T
$\frac{1}{\sigma}\frac{d\sigma}{dT}$
$\sqrt{q^2}$ = 20 GeV
10
1
0.1
U
L=2T
B
I
A
0.65
0.7
0.8
0.9
1
T

Fig. 4